Applied Catalysis B: Environmental 150–151 (2014) 432–437

Contents lists available at ScienceDirect

Applied Catalysis B: Environmental

journal homepage: www.elsevier.com/locate/apcatb

Unprecedented photocatalytic activity of carbonized leather skin residues containing chromium oxide phases

Juan C. Colmenares[a,*], Paweł Lisowski[a], Jose M. Bermudez[b,c], Jaume Cot[d], Rafael Luque[b,**]

[a] Institute of Physical Chemistry, Polish Academy of Sciences, ul. Kasprzaka 44/52, 01-224 Warsaw, Poland
[b] Departamento de Química Orgánica, Universidad de Córdoba, Edif. Marie Curie, Ctra Nnal IV-A, Km 396, E14014 Córdoba, Spain
[c] Instituto Nacional del Carbón, CSIC, Apartado 73, 33080 Oviedo, Spain
[d] Institut de Quiımica Avancada de Catalunya (IQAC) – Consejo Superior, de Investigaciones Cientıficas (CSIC), C/ Jordi Girona, 18-26, 08034 Barcelona, Spain

ARTICLE INFO

Article history:
Received 15 November 2013
Received in revised form
17 December 2013
Accepted 19 December 2013
Available online 27 December 2013

Keywords:
Leather skin residues
Photocatalysis
Chromium oxide
Phenol degradation

ABSTRACT

Carbonaceous N-containing materials derived from leather skin residues have been found to have unprecedented photocatalytic properties as compared to P25 Evonik, with an interesting degradation potential for contaminants in water (e.g. phenol). The carbonaceous materials were prepared by carbonization of the leather skin residues at different temperatures (180–600 °C). Different crystalline species of Cr_2O_3 and TiO_2 were found in the materials obtained. In spite of a low surface area and phase crystallinity, a thermally treated material at 180 °C containing doped chromium oxides (eskolaite phase) provided remarkably improved activities with respect to classical titania derived materials.

1. Introduction

One of the main focuses of present and future scientific research efforts is the development of improved manufacturing processes aiming to minimize environmental impact combined with maximum efficiencies [1]. Advanced waste valorization practises, beyond basic waste management practises currently implemented, can offer important advantages and a sustainable alternative for the production of chemicals, materials and fuels. In addition, they can play a key role in process enhancement giving rise to more environmental friendly processes and better economic balances [2,3].

Particularly, the meat and leather industries generate staggering volumes of residues that have attracted a significant deal of attention from scientists in recent years, as highlighted from the increase in scientific publications on these topics (Fig. 1). The leather industry produces remarkable amounts of waste (>800,000 tons/year worldwide) of two main different types including the so-called unusable wet blue (ca. 650,000 tons/year) as well as dry waste (e.g. trimmings and dust at ca. 150,000 tons/year of dry waste) [4]. Landfill disposal is the usual way to manage them, although new valorizing technologies are arising [5]. Spain has an important leather industry, mainly located in Catalonia and Andalucia.

These residues have currently no other exploitation different from landfilling, representing a significant environmental issue due to the presence of considerable amounts of transition metals in some of these residues (e.g. chromium, titanium) from different treatments such as tanning. Interestingly, a planned valorization of such metal-containing leather residues could lead to potentially interesting materials with applications in (photo)catalysis.

In the field of photocatalysis, the use of composites of carbonaceous materials and conventional TiO_2 photocatalysts has been the subject of several recent studies, due to the enhancement in photocatalytic properties provided by the interaction of TiO_2 with carbon containing materials [6]. Furthermore, N-doping is also a commonly extended and investigated practice in the development of light-visible nanomaterials due to the possibility to reduce the band gap of titania to act as efficient solar-driven photoactive material [7]. The photochemical activity of certain carbon materials in the absence of conventional photocatalysts under UV radiation has also been recently demonstrated [8,9].

In the light of these premises, the valorization of metal containing-leather skin residues by means of carbonization processes can be a potentially attractive way to synthesize C- and

* Corresponding author.
** Corresponding author. Tel.: +34 957211050; fax: +34 957782581.
E-mail addresses: jcarloscolmenares@ichf.edu.pl (J.C. Colmenares), q62alsor@uco.es (R. Luque).

0926-3373/$ – see front matter © 2013 Elsevier B.V. All rights reserved.
http://dx.doi.org/10.1016/j.apcatb.2013.12.038

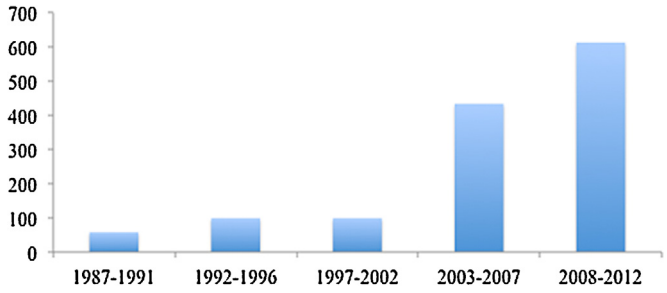

Fig. 1. Scientific publications dealing with leather waste residues. Source: Scopus.

N-containing metal oxides (including chromium and titanium oxides) with potentially envisaged photocatalytic properties. In fact, we have recently developed a proof of concept methodology to valorize processed and unprocessed leather residues to potentially interesting biomaterials for a series of applications from previous collaborations with meat and leather industries [10–14]. These included bio-collagenic materials for biomedical applications in tissue regeneration and CO_2 sequestration materials [12–14].

In the present work, we report the development of simple low temperature carbonization strategies for the preparation of carbonaceous N-containing (from proteins ubiquitous in animal skin) photocatalysts from leather skin residues that have been found to be efficient and highly active materials in the degradation of contaminants (e.g. phenol) under near UV-light irradiation.

2. Experimental

Leather skin residues were leftover trimmings from processed leather to bags, wallets and related consumer products kindly donated by Serpelsa S.A. from Vic (Barcelona). The original feedstock is rabbit skin. Samples are referred to PT (for processed skin) and numbered (1 and 2) depending on the type of sample and treatment. PT1 was processed under conventional and most extended chromium salt treatment, typical of over 80% of the leather processing industry while PT2 was processed and cured using titanium salts. Different batches were also processed in this work, showing a high reproducibility in terms of textural and adsorption properties.

Carbonisation of the leather residues was conducted in a microactivity reactor (PID, Spain) at three different temperatures (180, 200 and 350 °C) as well as at 600 °C only for structural and comparative phase purposes (XRD results). Reduced temperatures of carbonisation (<200 °C) lead to materials that had very similar properties to those of the original processed leather skin with nevertheless very different photocatalytic activities.

In a typical and simple carbonisation process, 2–3 g leather skin cut in small pieces were placed into the microactivity reactor and heated up at the desired temperature (from 180 to 350 °C) under a flow of nitrogen (50 mL/min) at 10 °C/min and then final stabilization at the carbonisation temperature for 60 min. The final carbonaceous material was then obtained upon cooling down of the system and processed accordingly.

2.1. Characterization of materials

Materials were characterized by means of several techniques including nitrogen physisorption, X-ray diffraction (XRD) and UV–vis spectroscopy.

XRD patterns were recorded on a Bruker AXS diffractometer with CuKα (λ = 1.5418 Å), over a 2θ ranged from 5 to 80°, using a step size of 0.01° and a counting time per step of 20 s.

Nitrogen adsorption measurements were carried out at 77.4 K using an ASAP 2010 volumetric adsorption analyzer from Micromeritics. The samples were outgassed 24 h at 150 °C under vacuum ($p < 10^{-2}$ Pa) and subsequently analyzed. The linear part of the BET equation (relative pressure between 0.05 and 0.30) was used for the determination of the specific surface area. D_{BJH} = mean pore size diameter; V_{BJH} = pore volumes. The pore size distribution was calculated from the adsorption branch of the N_2 physisorption isotherms and the Barrett–Joyner–Halenda (BJH) formula. The cumulative pore volume V_{BJH} was obtained from the pore size distribution (PSD) curve.

Ultraviolet–visible diffuse reflectance spectroscopy was performed using a UV-2501PC Shimadzu spectrophotometer. Band-gap values were calculated based on the Kubelka–Munk functions [15] $f(R)$, which are proportional to the absorption of radiation, by plotting $[f(R)hv)]^{1/2}$ against hv. The function $f(R)$ was calculated using Eq. (1):

$$f(R) = \frac{(1-R)^2}{2R} \quad (1)$$

Band gap values were obtained from the plot of the Kubelka–Munk function $[F(R_\infty)E]^{1/2}$ versus the energy of the absorbed light E. Regarding absorption threshold, it was determined according to the formula [16]:

$$\lambda = \frac{1240}{E_{gap}} \quad (2)$$

2.2. Photocatalytic experiments

All photocatalytic reactions were performed in a Pyrex cylindrical double-walled immersion well reactor with a total volume of 450 mL. The bath reactor was magnetically stirred to obtain a homogeneous suspension of the catalyst. A medium pressure 125 W mercury lamp (λ_{max} = 365 nm), supplied by Photochemical Reactors Ltd. (Model RQ 3010) was placed inside the glass immersion well as light irradiation source. The reaction temperature was set at 30 °C.

Phenol solution (50 ppm) was prepared in Milli-Q water. Experiments were conducted from 150 mL of the mother solution and 1 g/L of catalyst concentration was used. All reactions were carried out under ambient air (no oxygen bubbling conditions). Approximately 2 mL of samples was periodically taken from the photoreactor at specified times of reaction and filtered through 0.2 μm, 25 mm nylon filters in order to remove the photocatalyst prior to analysis. Phenol degradation was measured, after external standard calibration, by HPLC (Waters HPLC Model 590 pump), equipped with a PDA detector. Separation was performed on an XBridge™ C18 5 μm 4.6 mm × 150 mm column provided by Waters. The mobile phase was Milli-Q water/methanol (65:35, v/v) mixture with 0.1% of CF_3COOH at a flow rate of 1 mL/min. The injection volume was 10 μL. Blank experiments were performed in the dark as well as with illumination and no photocatalyst, without observable change in the initial concentration of phenol in both cases.

The degradation rate can be expressed as first-order with respect to the concentration of phenol:

$$r = \frac{-dC}{dt} = k_{app} * C \quad (3)$$

where k_{app} is the apparent rate constant of a pseudo first order reaction [17]. Integral form of reaction rate can be described as:

$$\ln\left(\frac{C_o}{C}\right) = k_{app} * t \quad (4)$$

where C_o is the initial phenol concentration and C is the concentration of phenol at time t.

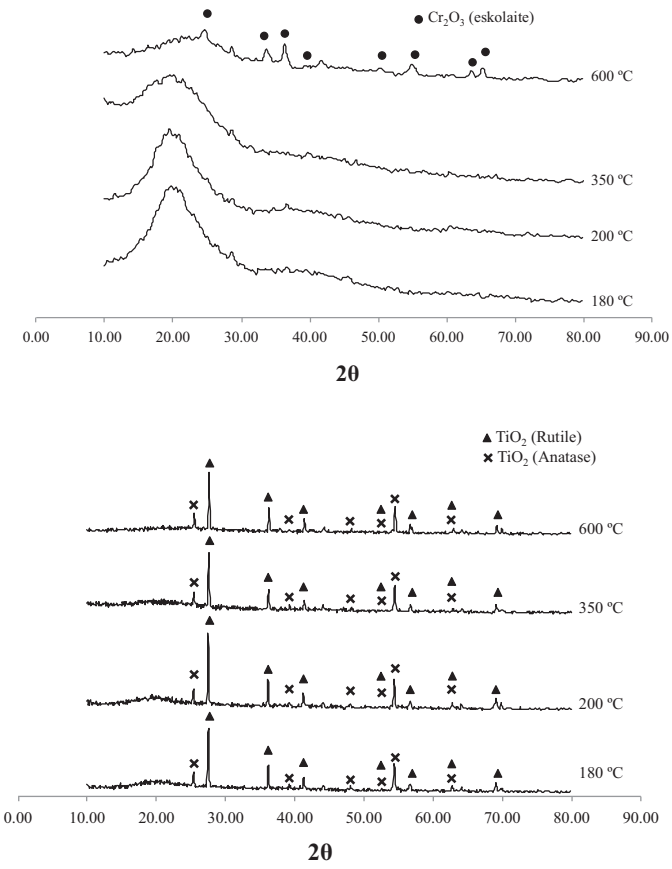

Fig. 2. XRD patterns of PT1 (top set) and PT2 (bottom set) materials carbonized under nitrogen at 180, 200, 350 and 600 °C.

By plotting $\ln(C_o/C)$ versus t, the apparent rate constant (k_{app}) can be determined from the slope of the regression line and these have been quantitatively presented in Table 2.

The percentage of phenol degradation ($D\%$) was calculated as follows:

$$D\% = \frac{C_o - C}{C_o} \quad (5)$$

Extraction was performed in order to determine the amount of phenol residual on the material surface after 240 min in the dark [18]. For this purpose, the photocatalyst was filtered and phenol extraction was carried out at 20% acetonitrile solution under ultrasound for 20 min.

3. Results and discussion

Leather residues carbonized under air showed the typical small mass loss associated to physisorbed water (ca. 100–110 °C, <10% mass loss) which was followed by a highly exothermic band between 300 °C and 480 °C, corresponding to the decomposition and burning of the residue into CO_2 and water as well as some NO_x species (see ESI, also in good agreement with TG/MS results, not shown), with a mass loss of over 70%) [12–14]. In the light of these results, samples were carbonized at three different temperatures (180, 200 and 350 °C) as well as a high temperature 600 °C material (just for structural comparative purposes) and compared to the parent skin materials in the photocatalytic application.

XRD patterns of carbonaceous materials obtained from processed leather residues (Fig. 2) pointed out the existence of the typical amorphous phase corresponding to a carbonaceous material (broad band at ca. $2\theta = 20°$, Fig. 2 top) for high temperature carbonized materials. Several crystalline peaks corresponding to the various species present in the leather skin residue could be observed in the XRD patterns (Fig. 2).

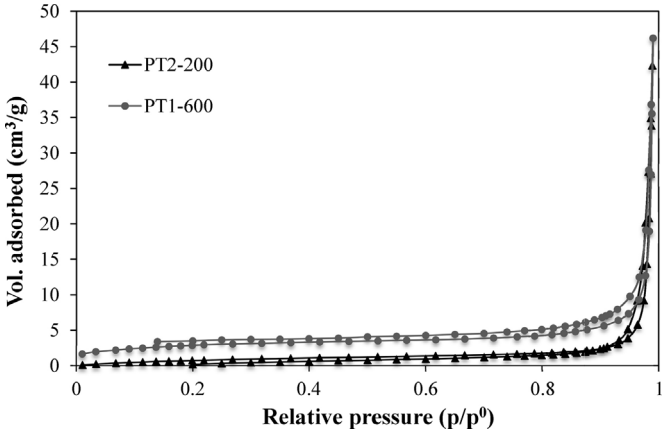

Fig. 3. N_2 adsorption isotherms of PT1-600 and PT2-200, selected as best materials in terms of textural properties for comparative purposes.

Diffraction lines corresponded to a chromium oxide eskolaite phase (Cr_2O_3) for PT1 and a titanium combined rutile and anatase phase of TiO_2 for PT-2 (Fig. 2). In the case of PT1, the eskolaite Cr_2O_3 phase was not evidenced at temperatures below 400 °C (Fig. 2A). Comparatively, the rutile phase was found in larger proportion as compared to the anatase phase in PT2 materials (Fig. 2). A remarkable finding of this work was the presence of a well-crystallized rutile phase (for PT2 samples, Fig. 2b), knowing that the thermodynamic phase transformation from anatase to rutile starts at temperatures higher than 600 °C [19]. This phase transformation might be influenced by the complex composition of the leather skin residues in terms of C and N content. Cr and Ti contents in the materials were measured by ICP-MS, showing <5 wt.% Cr and Ti (ca. 4.6 wt.%) in the investigated materials.

Nitrogen adsorption isotherms collected at 77.4 K do not generally show any signs of porosity in the materials, being predominantly non-porous (Fig. 3). The steep increase observed at high relative pressure is typically associated with either a macroporous structure or agglomerated small particles (interparticular macroporosity). The absence of any measurable microporosity by classic N_2 adsorption at 77.4 K (at first sight contradictory to the high CO_2 adsorption capacity observed in the materials) [14] is however well known from both carbon [20–22] and polymer research [23]. It points to the presence of ultrasmall pores, which cannot be easily filled by nitrogen at 77.4 K either due to size or kinetic restrictions. Table 1 summarizes the specific surface areas and pore volumes of the carbonized material.

Fig. 4 displays the UV–vis adsorption spectra of all prepared waste-derived photocatalysts in this work as compared to commercially available P25 Evonik photocatalyst. PT1 treated materials did not exhibit significant differences in UV spectra with regards to thermal treatments from 180 to 350 °C. PT1-200 exhibits a broad

Table 1
Porosity properties of carbonized materials investigated in this work.

Material	S_{BET} (m^2/g)	Pore volume (cm^3/g)
PT1	–	–
PT1-180	<5	–
PT1-200	<5	–
PT1-350	<5	–
PT1-600	10	0.05
PT2	–	–
PT2-200	<10	0.04

Table 2
Apparent rate constant (k_{app}) of phenol degradation for the synthesized catalysts.

Catalyst	After 20 min		After 240 min		Degradation (%)after 240 min
	k	R^2	K	R^2	
PT1-180	0.0028	0.9678	0.0031	0.9968	52
PT1-200	0.0014	0.8525	0.0020	0.9959	39
PT1-200-Repeat test	**0.0008**	**0.8358**	**0.0013**	**0.9940**	36
PT1-350	0.0031	0.9927	0.0025	0.9996	46
PT2-200	0.0023	0.9601	0.0011	0.9895	24
PT-2	0.0016	0.9916	0.0010	0.9944	24
PT-1	0.0011	0.8524	0.0016	0.9945	32
P25 Evonik	0.0245	0.9950	From 20 min to 240 min of illumination 0.0009	0.9780	37

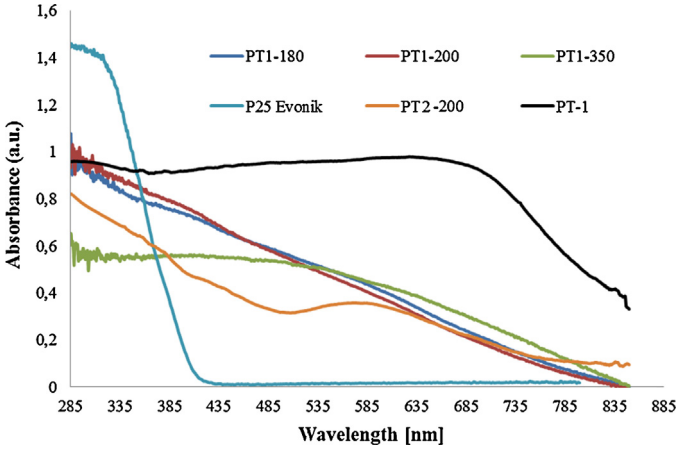

Fig. 4. Comparison of absorption spectra of PT1-180, PT1-200, PT1-350, PT2-200 as compared to their parent PT1 and PT2 as well as P25 Evonik.

absorption bands from 280 to 850 nm with respect to P25 Evonik. The band gap energy of sample is estimated from the $(\alpha h\nu)^{1/2}$ vs. photon energy plots to be 2.59 eV for PT2-200 (Fig. 5). However, interesting differences were observed of carbonized materials as compared to their parent PT1 and PT2 (Fig. 4).

Further characterization by XPS was conducted (results not shown) pointing out the structural complexity of the systems, that included several C and N contributions in the different spectra. N content measured by XPS was ca. 5%, while C was over 20%. Metal content was also estimated, showing relatively good agreement values (between 6 and 8% of Cr and Ti) in the investigated materials.

Phenol degradation efficiency results for the different carbonaceous leather residual materials are shown in Fig. 6. The most efficient phenol degradation was observed for material PT1-180, a most remarkable finding taking into account the presence of

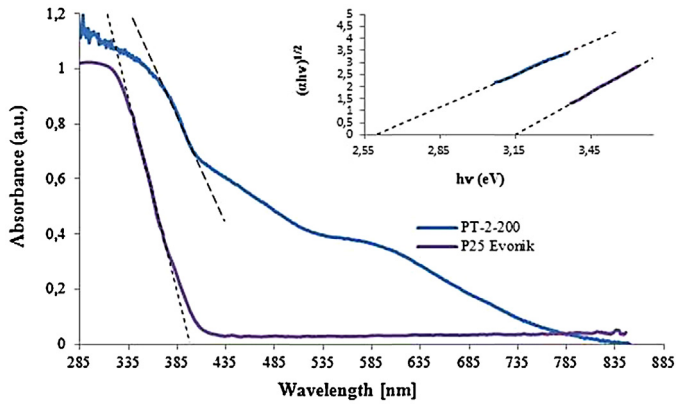

Fig. 5. UV–vis absorption spectra of PT2-200 and P25 Evonik.

the eskolaite Cr_2O_3 phase in the material. Almost 52% of phenol was degraded using PT1-180 (240 min irradiation), a significant difference as compared to untreated parent PT1 (<30% phenol degradation). Commercially available P25 Evonik showed the highest 25% initial phenol degradation activity up to approx. 25 min of illumination (Fig. 6), followed by only a slight increase in phenol degradation (up to 37%) after 240 min. A remarkable observation relates to the outstanding performance of PT1-180 even after only ca. 90 min photoreaction, comparably more active to P25 Evonik, in spite of its essentially non-porous nature (<5 m^2/g, Table 1) as compared to the relatively high porosity of P25 Evonik (50 m^2/g). No metal leaching from the photocatalysts (as demonstrated by ICP-MS measurements after the photocatalytic process) were in any case observed under the investigated conditions. Materials were also highly reproducible in terms of structure and photoactivity from batch to batch (see ESI for full details). These findings confirm the potential of these materials as stable photocatalysts for water detoxification (e.g. phenol removal).

Obtained results were also in good agreement with data from Figs. 7 and 8 as well as Table 2, which show the highest photoactivity in phenol degradation for PT1-180 (52% for removal rate and 0.0031 min^{-1} for rate constant after 240 min) under the investigated conditions.

Phenol degradation (D%) results are summarized in Table 2 and Fig. 8. With respect to a 52% highest degradation (PT1-180, 240 min light/catalyst exposure), PT1-350, PT1-200 and P25 Evonik degradations were 46, 39 and 37% under identical conditions, respectively. The lowest phenol degradation was 24% in the presence of PT2-200, which contains rutile as predominant titania phase. It is known that the adsorptive affinity of rutile for organic compounds (e.g. phenol) is lower to that of anatase and rutile exhibits higher rates of recombination electron–hole (lower photocatalytic activity) in comparison to anatase [24]. Results were also proved to be reproducible between batches and samples (Table 2, bold entries, see also ESI).

In any case, a contribution of phenol adsorbed under the investigated conditions could be present due to the nature of the photocatalytic materials. A detailed investigation of phenol adsorption studies in the absence of UV light was subsequently conducted as depicted in Fig. 9.

The amount of adsorbed phenol in the dark after 240 min was rather low for the different investigated catalysts (Fig. 9). Significantly larger quantities of phenol (2.6%) were adsorbed on PT2 materials as compared to PT1. The lowest phenol adsorption (1.2%) was observed for PT1-180, particularly the most active photocatalyst. These low phenol adsorption capacities can be well correlated to the negligible porosity and very low surface area of PT materials (Table 1).

High surface areas are an important factor in heterogeneous photocatalysis but generally not the most relevant. Other parameters including material crystallinity, phase composition, active center densities and also reactions conditions can

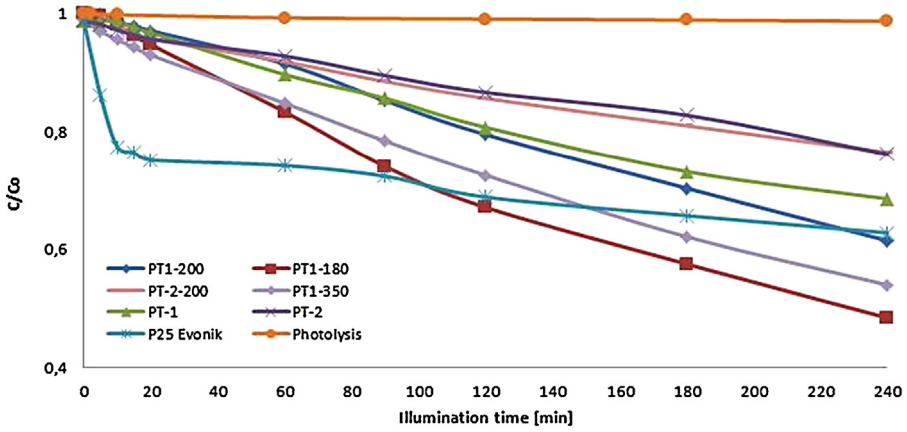

Fig. 6. Phenol degradation efficiency (measured as the relative concentration of phenol (C/C_o) over time) of various materials investigated in this work as compared to P25 Evonik.

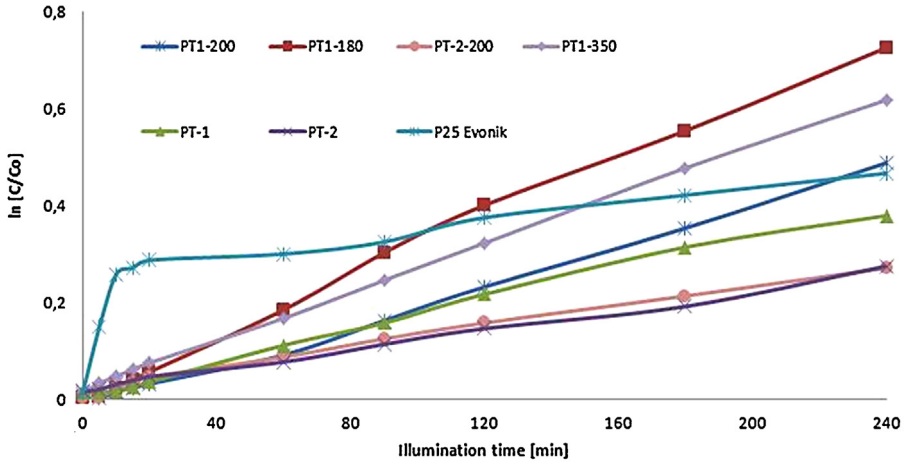

Fig. 7. Dependence of $\ln(C_o/C)$ on illumination time.

significantly influence photocatalytic activities in different systems. Based on current characterization data and the nature of the systems, we believe that PT1 carbonized materials (and particularly PT1-180) contain high density of photocatalytically active centers for phenol degradation, even at a low crystallinity and porosity, which together with C- and N-modification lead to excelling activities for photocatalytic phenol degradation as compared to P25 Evonik. Further characterization studies (including in situ and advanced XPS measurements as well as EXAFS studies) are currently ongoing aimed to a better understanding of the enhanced photocatalytic activity of the systems.

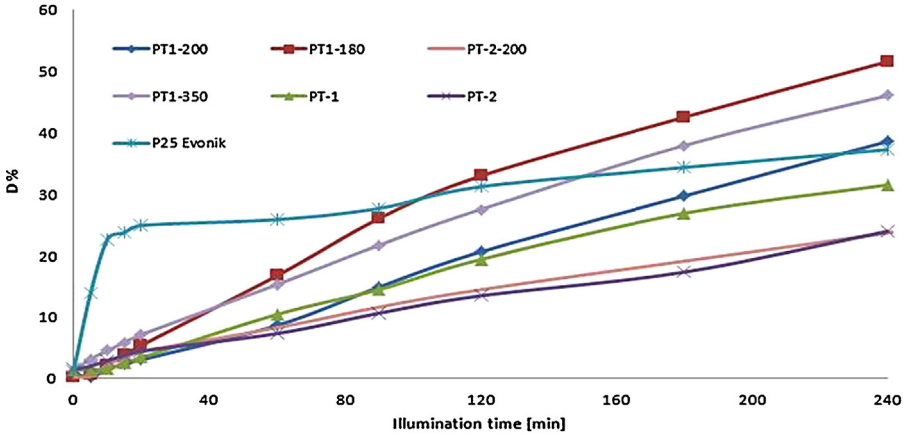

Fig. 8. Photocatalytic degradation curves of phenol for PT1 and PT2-derived materials and P25 Evonik.

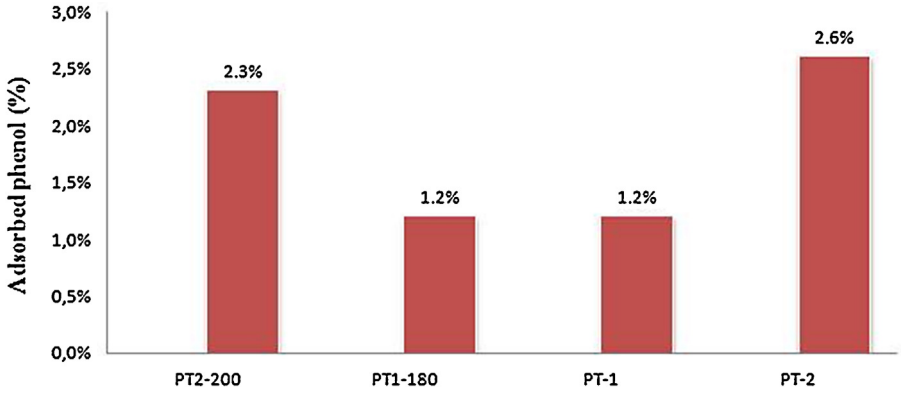

Fig. 9. Amount of phenol adsorbed for 240 min in the dark for catalysts.

4. Conclusions

Leather skin residues have been converted into useful carbonaceous materials that have very promising photocatalytic activities in the degradation of pollutants in water (e.g. phenol). Particularly, essentially non-porous low thermally treated materials containing low crystalline Cr_2O_3 eskolaite phases were proved to have unprecedented near UV photocatalytic activities toward phenol degradation as compared to a commercially available P25 Evonik. Highly photoactive low temperature materials can therefore be produced from inexpensive waste even with low burn-off rates and low temperature thermal treatments as opposed to equally performing sophisticated and carefully designed materials. The obtained results can be considered as rather competitive and encouraging to previous literature reports. The proposed materials are envisaged to be utilized in related photocatalytic processes under visible light irradiation, currently under investigation in our laboratories.

Acknowledgments

Rafael Luque gratefully acknowledges support from the Spanish MICINN via the concession of a RyC contract (ref. RYC 2009-04199) and funding under projects P10-FQM-6711 (Consejeria de Ciencia e Innovacion, 363 Junta de Andalucia) and CTQ2010-18126 and CTQ2011 364 28954-C02-02 (MICINN). Jose M Bermudez acknowledges the support received from the CSIC JAE Program. J.C. Colmenares wants to thank for the Marie Curie International Reintegration Grant within the 7th European Community Framework Programme and also the 2012–2014 science financial resources, granted for the international co-financed project implementation (Project Nr. 473/7.PR/2012, Ministry of Science and Higher Education of Poland).

References

[1] R. Constanza, H.E. Daly, Conserv. Biol. 6 (1992) 37–46.
[2] C.O. Tuck, E. Pérez, I.T. Horváth, R.A. Sheldon, M. Poliakoff, Science 337 (2012) 695–699.
[3] C.S.K. Lin, L. Pfaltzgraff, L. Herrero-Davila, E.B. Mubofu, S. Abderrahim, J.H. Clark, A. Koutinas, N. Kopsahelis, K. Stamatelou, F. Dickson, S. Thankappan, Z. Mohamed, R. Brocklesby, R. Luque, Energy Environ. Sci. 6 (2013) 426–464.
[4] http://www.unido.org/fileadmin/import/userfiles/timminsk/leatherpanel14ctcwastes.pdf
[5] R.R. Gil, R.P. Girón, M.S. Lozano, B. Ruiz, E. Fuente, J. Anal. Appl. Pyrolysis 98 (2012) 129–136.
[6] R. Leary, A. Westwood, Carbon 49 (2011) 741–772.
[7] R. Asahi, T. Morikawa, T. Ohwaki, K. Aoki, Y. Taga, Science 293 (2001) 269.
[8] L.F. Velasco, J.B. Parra, C.O. Ania, Appl. Surf. Sci. 256 (2010) 5254–5258.
[9] L.F. Velasco, I.M. Fonseca, J.B. Parra, J.C. Lima, C.O. Ania, Carbon 50 (2012) 258–259.
[10] M. Catalina, A.P.M. Antunes, G. Attenburrow, J. Cot, A.D. Covington, P.S. Phillips, J. Solid Waste Technol. Manage. 33 (2007) 43–50.
[11] M. Catalina, G.E. Attenburrow, J. Cot, A.D. Covington, A.P.M. Antunes, J. Appl. Polym. Sc1. 119 (2011) 2105–2111.
[12] M. Catalina, J. Cot, A.M. Balu, J.C. Serrano-Ruiz, R. Luque, Green Chem. 14 (2012) 308–312.
[13] M. Catalina, J. Cot, M. Borras, J. De Lapuente, J. Gonzalez, A.M. Balu, R. Luque, Materials 6 (2013) 1599–1607.
[14] J.M. Bermudez, P. Haro-Dominguez, A. Arenillas, J. Cot, J. Weber, R. Luque, Materials 6 (2013) 4641–4653.
[15] S. Sakthivel, H. Kisch, Angew. Chem. Int. Ed. 42 (2003) 4908–4911.
[16] H.-S. Lee, C.-S. Woo, B.-K. Youn, S.-Y. Kim, S.-T. Oh, Y.-E. Sung, H.-I. Lee, Top. Catal. 35 (2005) 3–4.
[17] N.A. Laoufi, D. Tassalit, F. Bentahar, Global NEST J. 10 (2008) 404–418.
[18] Y. Ao, J. Xu, D. Fu, X. Shen, Ch. Yuan, Colloids Surf. A: Physicochem. Eng. Aspects 312 (2008) 125–130.
[19] H. Xie, Q. Zhang, T. Xi, J. Wang, Y. Liu, Thermochim. Acta 381 (2002) 45.
[20] F. Rodriguez-Reinoso, J.D. Lopez-Gonzalez, C. Berenguer, Carbon 20 (1982) 513–518.
[21] D. Lozano-Castelló, D. Cazorla-Amoros, A. Linares-Solano, Carbon 42 (2004) 1231–1236.
[22] L. Yu, C. Falco, J. Weber, R. White, J.Y. Howe, M.M. Titirici, Langmuir 28 (2012) 12273–12283.
[23] N. Ritter, I. Senkovska, S. Kaskel, J. Weber, Macromolecules 44 (2011) 2025–2033.
[24] U. Stafford, K.A. Gray, P.V. Kamat, A. Varma, Chem. Phys. Lett. 205 (1993) 55.